THE TOPOLOGY OF INTERMEDIATE MASS FRAGMENT EMISSION.

W. J. LLOPE[§]
T.W. Bonner Nuclear Laboratory
Rice University
Houston, TX, 77251-1892

ABSTRACT

The study of the patterns in momentum and/or coordinate space, i.e. the topology, of fragment emission in central heavy-ion collisions allows one to distinguish between the sequential binary (SB) and multifragmentation (MF) disassembly modes. We present results on fragment azimuthal correlations using two different methods, and each implies beam energy dependent transitions between these two disassembly modes. An experimental data set consisting of 40 reactions in the entrance channels ^{12}C+^{12}C, ^{20}Ne+^{27}Al, ^{40}Ar+^{45}Sc, ^{84}Kr+^{93}Nb, and ^{129}Xe+^{139}La was used for these analyses, as well as our previous studies of central event topology using the sphericity variable. The SB to MF transitional behavior extracted from all of these analyses will be compared to independently measured disassembly time scales. It will be shown that, for increasing energies, the SB to MF transitions that we observe occur at energies consistent with those leading to strong decreases in the disassembly time scales. This lends credence to the identification that the present SB to MF transitions are the physical manifestation of a nuclear liquid-gas phase transition.

1. Introduction

The identification of the liquid and gaseous phases of some excited thermodynamic system of A particles via the characteristics of its disassembly is straightforward. Excited liquids evaporate, or undergo fission, while gases rapidly expand to fill their container. The application of such classical concepts for the understanding of the excited systems formed in heavy-ion collisions is made difficult by the quantum-mechanical nature and charge, Z, of these systems, as well as the fact that A is some twenty-three orders of magnitude less than the thermodynamic limit. Detailed model calculations[1] nonetheless imply that the equivalent of a proper liquid-gas phase transition occurs in finite nuclear systems at excitation energies between

[§]For the MSU 4π Group: National Superconducting Cyclotron Laboratory, Michigan State University; T.W. Bonner Nuclear Laboratory, Rice University; Department of Chemistry, State University of New York - Stony Brook; Department of Physics, U. of Michigan - Dearborn; Cyclotron Institute, Texas A&M University; Department of Physics and Astronomy, U. of Iowa.

$\sim$4 to $\sim$10 MeV/nucleon, depending on A and Z. Experimental searches for such a phase transition are complicated by pre-equilibrium emission, non-zero angular momenta, and the inability to strictly control Z, A, and the excitation energy via the impact parameter. Systematic experimental data sets collected using a nearly hermetic apparatus allow one to overcome such effects, and to search for the nuclear liquid-gas phase transition. One compelling signal of the nuclear gaseous phase following the central collision of two nuclear liquids at intermediate beam energies is the observation of extremely short disassembly time scales,[2] i.e. $\lesssim$100 fm/c. Indeed, a number of experiments[3,4] have observed *decreasing* time scales with increases in the beam energy over the range from some tens to $\sim$100 MeV/nucleon.

Beam energy dependent transitions from Sequential Binary (SB) disassembly to multifragmentation (MF) also appear in this beam energy range for central collisions.[5] Sequential binary disassembly proceeds via a cascade of two-body decay steps, which in many ways resembles the dissociation of an excited liquid. For excitation energies above $\sim$1-2 MeV/nucleon and the typical angular momenta involved in central heavy-ion collisions, the initial stage of this disassembly mode involves an (a)symmetric fission, which results in two excited pre-fragments moving back-to-back in the rest frame of the decaying system. These pre-fragments may, depending on the excitation energy, subsequently undergo further fissions or particle evaporation. Overall, the largest fragments in the final state reflect the back-to-back emission of the two primordial pre-fragments. On the other hand, multifragmentation proceeds via a more violent "explosion" of the excited nucleus. This mode produces more than two excited pre-fragments, which may evaporate particles as they rapidly move apart under strong inter-particle Coulomb repulsions. The largest fragments in the final states of this mode of disassembly are more isotropically distributed in the rest frame of the decaying system.

The study of the topology, i.e. the patterns in momentum and/or coordinate space, of intermediate mass fragment (IMFs, for which $3 \leq Z \lesssim 20$) emission can therefore distinguish between the SB and MF scenarios.[6] In previous work, we have obtained evidence for SB to MF transitions using many different experimental observables in a systematic set of experimental data.[7,8,9,10] The majority of this evidence was obtained from the study of the fragment topology in a momentum space coordinate system that spatially coincides with the center of momentum (CM) frame as quantified by the sphericity variable.[8,10] In this Contribution, additional evidence for SB to MF transitions is presented, which was obtained from the study of the fragment coordinate space topology via the quantification of the IMF azimuthal distributions. Two different methods will be described. The SB to MF transitional beam energies that are extracted will be compared with the transitional energies that were implied by the previous analyses.

Of principal interest is the evaluation of the extent to which the observed SB to MF transitions are indeed a reflection of a nuclear liquid-gas phase transition.

To this end, we will finally describe the comparison of the SB to MF transitional energies that we observe with the independently measured time scales for the disassembly of the excited systems formed in the same or similar central reactions.

The experimental data were collected with the Michigan State University 4π Array[11] at the National Superconducting Cyclotron Laboratory (NSCL) using beams extracted from the K1200 cyclotron. The reactions that were studied include ^{12}C+^{12}C at 55, 75, 95, 105, 115, 125, 135, 145, and 155 MeV/nucleon, ^{20}Ne+^{27}Al at 55, 75, 95, 105, 115, 125, 135, and 140 MeV/nucleon, ^{40}Ar+^{45}Sc at 15, 25, 35, 45, 65, 75, 85, 95, 105, and 115 MeV/nucleon, ^{84}Kr+^{93}Nb at 35, 45, 55, 65, and 75 MeV/nucleon, and ^{129}Xe+^{139}La at 25, 30, 35, 40, 45, 50, 55, and 60 MeV/nucleon. Detailed information on the data collection may be found elsewhere.[3,7,8,9,10,12,13]

2. Transitions as viewed by azimuthal correlations

The study of the opening angles between the largest fragments in the final states of central heavy-ion reactions should provide a clear separation between the SB and MF disassembly modes[6]. By assumption, SB disassembly results in larger average opening angles between the two heaviest fragments as compared to those following MF. The calculation of fragment opening angles in the rest frame of the decaying system, however, involves the assumption of the laboratory velocity of this system. For the most central collisions, this source velocity could be assumed to be the velocity of the CM frame, or experimentally measured as the weighted average of the components of the final state particle velocities along the beam direction. The study of the relative *azimuthal* angles of the emitted fragments in such reactions has the advantage that the specification of a source velocity is not necessary. Furthermore, the effects of the experimental acceptance on a study of relative azimuthal angles are of little concern if an azimuthally symmetric apparatus, e.g. the MSU 4π Array, was used to collect the data. If the selection of central collisions is sufficiently strict, the contributions from directed transverse flow[12,13] and collective rotational motion[13] are strongly suppressed. This allows the one to assume that central events with azimuthally back-to-back heavy fragments follow SB disassembly, while those with azimuthally isotropic fragments follow MF.

The central events were selected by a two-dimensional cut on the total transverse kinetic energy and the total mid-rapidity charge, giving $b_{max}{\sim}0.2[R_P + R_T]$ geometrically. This cut is significantly more central than that used in Refs. 12 and 13, where the contributions of transverse directed flow and rotational motion were observed in the same data set studied herein. This centrality cut does not autocorrelate[7] with the analyses described in the following two Sections.[9]

2.1. Azimuthal correlations of the three heaviest fragments

The relative azimuthal angles of the three largest fragments in each central event, $\Delta\phi_i$, are measured in such a way that $\sum \Delta\phi_i = 1$. The events are plotted *a lá*

Dalitz[14] in a triangle so that the perpendicular distances to each of the the three axes are $\Delta\phi_i$. Such plots of relative azimuthal angles are not affected by the "Z_{sum}" dependences intrinsic to the relative charge Dalitz plots.[9] The relative azimuthal angle Dalitz plots for the central ^{40}Ar+^{45}Sc and ^{129}Xe+^{139}La events are shown in Figure 1.

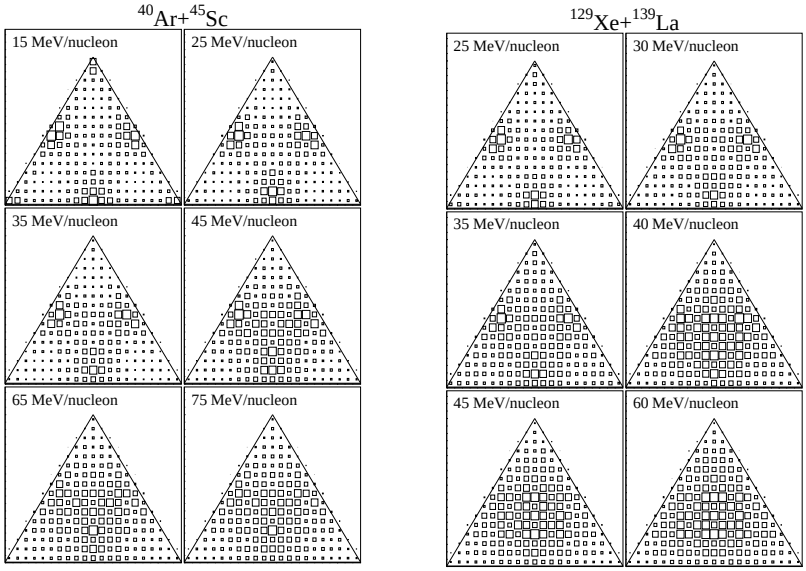

Fig. 1: The relative azimuthal angle Dalitz plots for the three largest fragments in the central ^{40}Ar+^{45}Sc and ^{129}Xe+^{139}La reactions at six different beam energies each.

Events near the corners of the triangles are those in which all three of the largest fragments have nearly the same laboratory azimuthal angle. Events populating the sides of these triangles include two nearly back-to-back fragments, with the third fragment relatively close in azimuthal angle to one of the other two. A population of events near the center have three fragments that are azimuthally isotropic.

At the lowest beam energies shown in Figure 1, a predominance of events near the sides of these triangles is apparent. As the beam energy is increased, both entrance channels shown an accompanying increase in the number of events near the centers of these triangles, and a depletion of the events near the sides. These plots are thus consistent with a transition from sequential binary disassembly to multifragmentation, as the data indicates a change from predominantly back-to-back heavy fragment emission to fragment azimuthal isotropy for increasing beam energies.

However, it is difficult to locate a transitional beam energy from the plots shown in Figure 1. To quantify these plots, we measure the values of the distances D^{ϕ}_{cent} and D^{ϕ}_{edge} for each central event. These variables were first used as a means of quantifying the relative charge Dalitz plots that were discussed in Ref. 9. The quantity $D^{\phi}_{cent}(D^{\phi}_{edge})$ is the distance from the position of the event in the triangle to the center(nearest edge). According to the assumptions above, a sample of predominantly

SB events has $\langle D^{\phi}_{cent}\rangle > \langle D^{\phi}_{edge}\rangle$, while a sample of MF events has $\langle D^{\phi}_{cent}\rangle < \langle D^{\phi}_{edge}\rangle$. A minimum in the beam energy dependence of the quantity $\langle D^{\phi}_{cent}\rangle$, with a maximum in the same dependence of $\langle D^{\phi}_{edge}\rangle$, indicates a beam energy at which the central events are maximally isotropic azimuthally.

The beam energy dependence of $\langle D^{\phi}_{cent}\rangle$ and $\langle D^{\phi}_{edge}\rangle$ is shown in Figure 2. The results for the central events for all of the available entrance channels and beam energies are shown with the different point styles as labelled in the Figure.

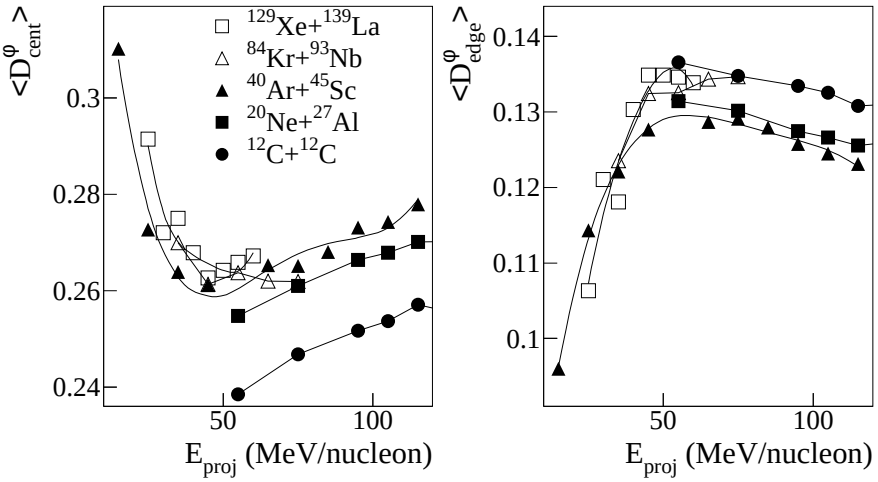

Fig. 2: The average values of D^{ϕ}_{cent} (left frame) and D^{ϕ}_{edge} (right frame) obtained from the relative azimuthal angle Dalitz plots versus the beam energy in the central events for the reactions listed in the left frame.

Relatively large(small) values of $\langle D^{\phi}_{cent}\rangle(\langle D^{\phi}_{edge}\rangle)$ are apparent at beam energies near and below ~35 MeV/nucleon. Minima(Maxima) in $\langle D^{\phi}_{cent}\rangle(\langle D^{\phi}_{edge}\rangle)$ are observed at beam energies near ~50 MeV/nucleon in the central ^{40}Ar+^{45}Sc reactions, and near ~45 MeV/nucleon in the central ^{129}Xe+^{139}La reactions. Consistent trends are observed for the other reactions. Above the beam energies leading to the minimal(maximal) values of $\langle D^{\phi}_{cent}\rangle(\langle D^{\phi}_{edge}\rangle)$, relatively more gradual increases(decreases) are observed for increasing beam energies. A SB to MF transitional beam energy near ~45 MeV/nucleon, depending slightly on the entrance channel mass, is therefore implied. An alternative means of quantifying the azimuthal distributions of the emitted fragments, which has two advantages as compared to the Dalitz method described above, is described in the next Section.

2.2. Azimuthal correlations of N_{IMF} fragments

The EMU01 Collaboration proposed[15] a pair of complementary observables for the study of the azimuthal patterns of particles emitted in 200 GeV/nucleon collisions at the CERN/SPS. We will apply these two observables to quantify azimuthal distributions in a way that differs somewhat from that used in Ref. 15. This method

has two important advantages over the Dalitz azimuthal correlations analysis described in the previous Section. First, the azimuthal patterns of the particle emission can be quantified for an arbitrary number of particles, and second, the mean values of each variable can be derived in the limit of purely stochastic emission of independent particles in a simple way for each multiplicity under consideration.

These variables are applied for the study of IMF emission in the present data by first measuring the azimuthal angles of the N_{IMF} fragments in a central event in the same way as done in the previous Section, i.e. so that $\sum_{i=1}^{N_{IMF}} \Delta\phi_i$=1. The variables S_1 and S_2 are then defined as:

$$S_1 = -\sum_{i=1}^{N_{IMF}} log(\Delta\phi_i), \quad \text{and} \quad S_2 = \sum_{i=1}^{N_{IMF}} \Delta\phi_i^2. \tag{1}$$

The variable $S_1(S_2)$ is large if there are small(large) gaps in the particle azimuthal distributions, implying "jet-like" azimuthal distributions according to Ref. 15. Thus, under the same assumptions used in the previous Sections, large values of these variables imply SB disassembly, while small values imply "ring-like" distributions,[15] indicating multifragmentation. The mean values of these variables in the purely stochastic limit are given by:

$$S_1^{stoch} = N_{IMF} \sum_{k=1}^{N_{IMF}-1} \frac{1}{k} \quad \text{and} \quad S_2^{stoch} = \frac{2}{N_{IMF}+1}. \tag{2}$$

The experimental distributions of S_1/S_1^{stoch} and S_2/S_2^{stoch} have been extracted from all of the present reactions and for all IMF multiplicities in the central events.

The truncated icosahedron, or "soccer ball", geometry of the MSU 4π Array has several groups of detectors with centers at different polar angles but the same azimuthal angle. Particle hits in two such detectors that are included in the calculation of S_1 and S_2 result in a divergence in the calculation of S_1. However, the variables S_1 and S_2 are complementary, like the variables D_{cent}^{ϕ} and D_{edge}^{ϕ}. We will therefore simply concentrate on the variable S_2 in the discussion below.

The experimental values of $\langle S_2\rangle/S_2^{stoch}$ versus the beam energy are shown in Figure 3. Mean values of this ratio that are below(above) unity imply azimuthal distributions that are more isotropic(planar) than the stochastic limit. In similarity to the results extracted in the previous Section, the ^{40}Ar+^{45}Sc results imply SB disassembly at beam energies below ~35 MeV/nucleon, as $\langle S_2\rangle/S_2^{stoch}$ exceeds unity. The results for the other reactions imply a universal trend with the beam energy. Minimal values of $\langle S_2\rangle/S_2^{stoch}$, i.e. maximal IMF azimuthal isotropy, occurs at beam energies near ~35-45 MeV/nucleon for N_{IMF}=3, and ~45-55 MeV/nucleon for $N_{IMF}\geq$5. These minima are below unity, i.e. the IMFs are more azimuthally isotropic than the stochastic average, which implies that the MF mechanism governed the disassembly at the beam energies near and above these minima.

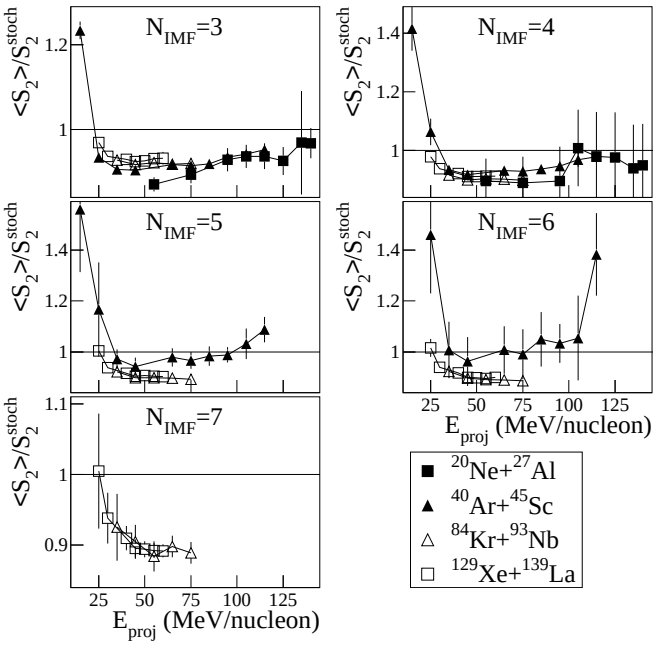

Fig. 3: The experimental values of $\langle S_2 \rangle / S_2^{stoch}$ versus the beam energy for the reactions listed on the lower right. The quantity S_2 is calculated only for the IMFs in the central events. Each frame corresponds to a specific IMF multiplicity as labelled.

3. Comparison to time scale measurements

The azimuthal correlations analyses of the previous Sections, and our previous studies of the topology of IMF emission,[8,10] imply SB to MF transitions for increasing beam energies in the central ^{40}Ar+^{45}Sc, ^{84}Kr+^{93}Nb, and ^{129}Xe+^{139}La reactions. The beam energies at which these transitions are observed are summarized in Figure 4. Also included in this Figure is the SB to MF transitional energies observed via a Dalitz charge correlations analysis of the present data,[9] and an event shape analysis of central ^{40}Ar+^{51}V reactions.[16] The transitional beam energies implied by all of the analyses for each reaction are quite similar, despite the fact that many different observables were studied. The transitional beam energies decrease from ~50 MeV/nucleon to ~40 MeV/nucleon, with increases in the entrance channel mass from ~80 to ~280, for reasons that were discussed in Ref. 10.

To evaluate the extent to which the observed SB to MF transitions are the physical manifestation of a nuclear liquid-gas phase transition, we compare the observed SB to MF transitional energies with independent measurements for the disassembly time scales.[3,4] These time scale measurements involved generally different symmetric and asymmetric entrance channels than those used for the results of Figure 4. Thus, to allow comparisons with the present results, the time-scales are plotted not as a function of the beam energy, but instead versus the excitation energy for each reaction obtained in the limit of perfectly inelastic collisions. This limiting excita-

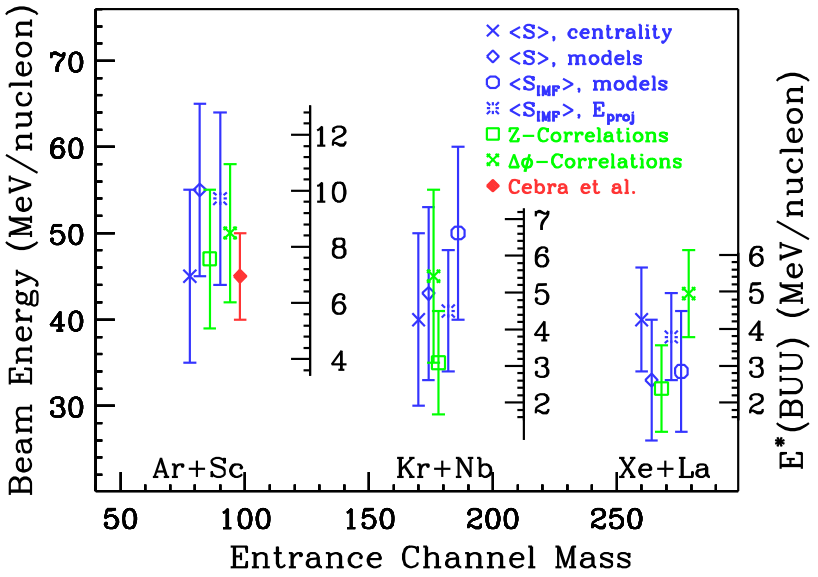

Fig. 4: The SB to MF transitional beam energies extracted from all of the analyses of the present data for the central ^{40}Ar+^{45}Sc, ^{84}Kr+^{93}Nb, and and ^{129}Xe+^{139}La reactions. The various analyses are described in Refs. 8,9,10, and in the previous Sections. Predictions for the excitation energies reached in these central reactions obtained from BUU calculations[7] are shown on the right-side axes.

tion energy is defined as $\frac{E_{proj}}{A_{proj}}\frac{\mathcal{V}_{CM}}{\mathcal{V}_{proj}}(1-\frac{\mathcal{V}_{CM}}{\mathcal{V}_{proj}})$, where E_{proj} is the beam energy, A_{proj} is the projectile mass number, and $\mathcal{V}_{CM}(\mathcal{V}_{proj})$ is the laboratory velocity of the CM frame(projectile).

The disassembly time scales from these independent measurements are shown in Figure 5. The present SB to MF transitional energies, i.e. Fig. 4, are enclosed in the shaded region, while the time scales in fm/c are shown as the large numbers, labelled by the various point styles. The time scale measurements shown in this Figure are representative of a larger number of such measurements that have been published. The measurements of Lisa *et al.* and Bauge *et al.* involved symmetric reactions measured with the MSU 4π Array, while the remainder of the results were obtained in asymmetric collisions measured with different detector systems. The results of Bauge *et al.* were in fact obtained from exactly the same ^{84}Kr+^{93}Nb reactions discussed in the previous Sections and in Refs. 7,8,9,10. For the other time scale measurements, the differences in the entrance channel nuclei and the experimental devices, as well as the different methods used to extract the time scales in each of these analyses, demand that the comparisons in Figure 5 be taken as qualitative only.

Central reactions populating the region below the shaded band in Figure 5 form excited systems that predominantly disassemble via the SB mechanism. The time scales for the reactions in this region are in the range from ~150 fm/c to ~500 fm/c. Above the shaded band, i.e. in the MF domain, time scales from ~30 fm/c to ~125 fm/c have been observed. Despite the caveats noted above, these trends imply

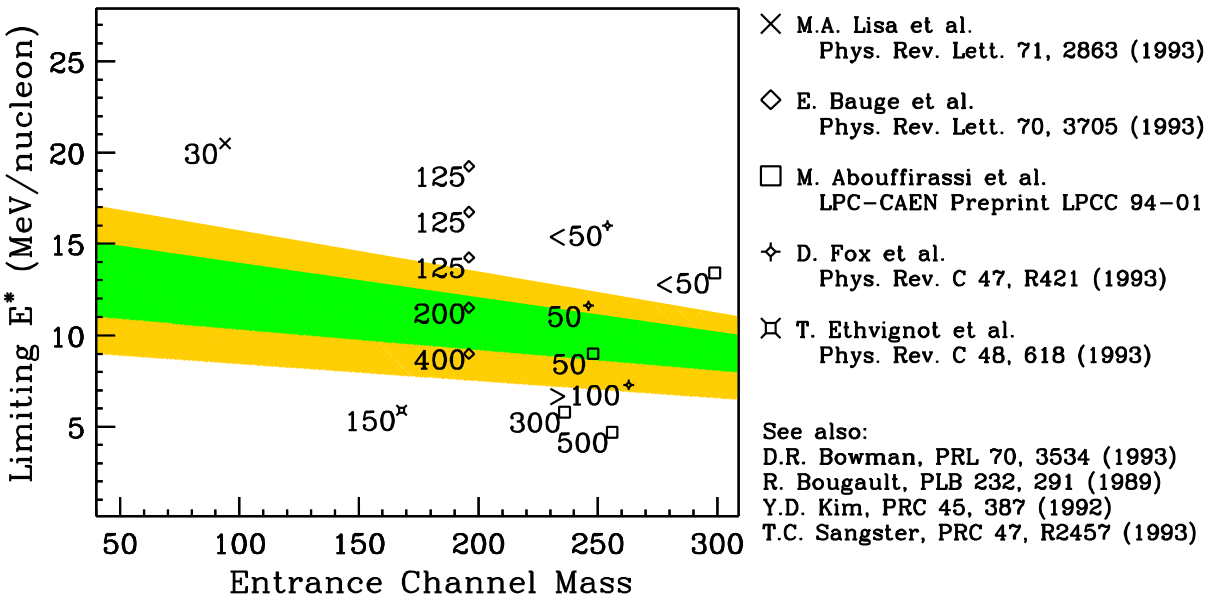

Fig. 5: The comparison of the SB to MF transitional energies, shown as the shaded region (from Fig. 4), with the independently measured time scales (in fm/c) for the same or similar reactions.[3,4] To allow this comparison, the present results and the time scales are plotted on the vertical axis using the limiting excitation energy (see text) for each projectile/target combination and beam energy.

that the SB to MF transitions observed in our analyses are indeed accompanied by significant decreases in the independently measured disassembly time scales. This lends credence to the identification that the present SB to MF transitions are indeed indicative of a nuclear phase transition from an excited quantum liquid phase to a phase of liquid-gas coexistence with disassembly time scales consistent with that of a quantum gas.

The present systematic results clearly indicate an entrance channel mass dependence of the transitional energies in central symmetric heavy-ion collisions.[10] The excitation energies for these transitions can be obtained from, e.g., BUU calculations,[7] and are ~8-10 MeV/nucleon for systems with A~70 and $\frac{Z}{A}$~0.5, and ~3-5 MeV/nucleon for systems with A~250 and $\frac{Z}{A}$~0.4. We note that the systems formed in the heavier symmetric collisions studied herein are generally more proton-rich than ground state nuclei of the same total mass. Further work should therefore concentrate on the dependence of the transition energy on the total charge, Z, of systems of fixed total mass, A. This will allow the disentangling of the presumably different dependences of the transition energies on the total mass and on the Coulomb energy in the excited system. Additional work should extend the systematics of the time scale measurements in such a way that the energy dependence of the disassembly time scales can be more quantitatively compared to the present results on SB to MF transitions.

4. Acknowledgements

We thank Thomas Glasmacher and M. Betty Tsang for helpful comments concerning time scale measurements. This work was supported by the U.S. Department of Energy under the Grant No. DE-FG03-93ER40772, and the U.S. National Science Foundation under Grants No. PHY 89-13815 and No. PHY 92-14992.

5. References

[1] J.P. Bondorf *et al.*, *Nucl. Phys.* **A448**, 753 (1986), and references therein; D.H.E. Gross, *Prog. Part. Nucl. Phys.* **30**, 155 (1993), and references therein; A.S. Botvina *et al.*, *Nucl. Phys.* **A475**, 663 (1987); W. Bauer, *Phys. Rev. C* **38**, 1297 (1988).

[2] S. Pratt and M.B. Tsang, *Phys. Rev. C* **36**, 2390 (1987).

[3] E. Bauge *et al.*, *Phys. Rev. Lett.* **70**, 3705 (1993).

[4] M.A. Lisa *et al.*, *Phys. Rev. Lett.* **71**, 2863 (1993); T. Ethvignot *et al.*, *Phys. Rev. C* **48**, 618 (1993); D. Fox *et al.*, *Phys. Rev. C* **47**, R421 (1993); M. Abouffirasi *et al.*, LPC-CAEN Preprint LPCC 94-01 (1994); D. Durand *et al.*, LPC-CAEN Preprint LPCC 94-02 (1994).

[5] L.G. Moretto and G.J. Wozniak, *Ann. Rev. Nucl. Part. Sci.* **43**, 379 (1993), and references therein; H. Fuchs and K. Möhring, *Rep. Prog. Phys.* **57**, 231 (1994), and references therein.

[6] J.A. López and J. Randrup, *Nucl. Phys.* **A491**, 477 (1989).

[7] W.J. Llope *et al.*, *Phys. Rev. C*, in press.

[8] W.J. Llope *et al.*, MSU Preprint MSUCL-959, *Phys. Rev. C*, submitted (1995).

[9] N.T.B. Stone, W.J. Llope, and G.D. Westfall, MSU Preprint MSUCL-916, *Physical Review C*, submitted (1994).

[10] W.J. Llope *et al.*, "Advances in Nuclear Dynamics, Proc. of the 10^{th} Winter Workshop on Nuclear Dynamics", eds. J. Harris, A. Mignerey, and W. Bauer, Snowbird, Utah (1994).

[11] G.D. Westfall *et al.*, *Nucl. Inst. and Methods* **A238**, 347 (1985).

[12] G.D. Westfall *et al.*, *Phys. Rev. Lett.* **71**, 1986 (1993).

[13] R.A. Lacey *et al.*, *Phys. Rev. Lett.* **70**, 1224 (1993); J. Lauret *et al.*, *Phys. Lett. B* **339**, 22 (1994).

[14] R.H. Dalitz, *Phil. Mag.* **44**, 1068 (1953); E. Fabri, *Nuovo Cim.* **11**, 479 (1954).

[15] M.I. Adamovich *et al.* (The EMU01 Collaboration), *J. Phys. G*, **19**, 2035 (1993); E. Stenlund *et al.* (The EMU01 Collaboration), *Nucl. Phys.*, **A498**, 541c (1989).

[16] D.A. Cebra *et al.*, *Phys. Rev. Lett.* **64**, 2246 (1990).